Electrical Power and Energy Systems 120 (2020) 106027

Contents lists available at ScienceDirect

Electrical Power and Energy Systems

journal homepage: www.elsevier.com/locate/ijepes

Partial discharges activated by impulses and superimposed voltages in a high voltage cable model

Jiayang Wu*, Armando Rodrigo Mor, Johan J. Smit

Delft University of Technology, Electrical Sustainable Energy Department, Mekelweg 4, 2628CD Delft, the Netherlands

ARTICLE INFO

Keywords:
High-voltage cross-linked polyethylene (XLPE)
cable model joint defect
Partial discharge (PD)
Impulse voltage
Superimposed voltage

ABSTRACT

In practice, High-voltage (HV) cables are occasionally exposed to impulse and superimposed transient conditions, which may initiate partial discharges (PD) temporarily. Whether such PDs persist under AC voltage after the transient conditions have vanished, is at focus in the research described in this paper. Since for cross-linked polyethylene (XLPE) cables the accessories are weak links in the HV cable insulation system, we investigated the PD behavior of an artificial joint defect in a HV cable model under impulse and superimposed voltages. By applying a dedicated PD measuring system it was found that, the impulse and superimposed voltages can initiate PD in the artificial defect, which under local electrical field conditions can persist for some time. The different parameters of the applied voltages have different effects on the PD behavior.

1. Introduction

By facing the expanding power grids, underground power cables are installed more and more as an alternative to overhead lines [1,2]. By 2006, 57% of all cables in service are cross-linked polyethylene (XLPE) insulated cable, and 70% of all accessories are extruded types [3]. Nowadays extruded cables, especially XLPE cables, increasingly dominate new installments. This is due to their higher efficiency brought by the lower dielectric constant, higher operating temperature and easier manufacturing and installation process [4].

A failure investigation based on approximately 170 individual power cables in service over the period from 1997 until 2014 [5], learned that around 69% of the failures occurred in the cable accessories. More than half of the failure causes of XLPE cables in the sample pool (74%) occurred in the cable accessories due to installation related defects. The latter weak link of the insulation system is at focus in the present experimental investigation about transient effects.

In service, power cable systems are occasionally subjected to abnormal superimposed transient conditions, where impulses are superimposed on the normal AC voltage. One example is a mixed overhead line and cable system, in which a switching action may lead to high frequency oscillations, causing large superimposed voltage impulses [6]. Cable systems are well designed to withstand the normal operating and transient conditions, however in such cases the insulation system faces exceptional superimposed transient overstress conditions.

Usually, most defects in the cable insulation are detected through PD test during commissioning tests or maintenance tests. However, it is well-known that the usual PD measurement techniques cannot detect all possible cable insulation defects [7,8]. In the above-mentioned case defects may exist, in which PDs are not detectable in maintenance or commissioning tests, while these may initiate at abnormal superimposed voltage conditions. In a worse case, possibly PDs may be initiated by the transient overvoltage, which continue under normal AC voltage. Therefore, it is important to know whether transient situations can initiate PD deteriorating the insulation, which could affect the functioning of the cable and its accessories, and what could be the partial discharge phenomena under transient conditions.

So far, PD phenomena under AC voltage have been widely studied. However, comparatively little has been written about PDs under impulse voltages and superimposed voltages. By evaluating PDIV, PDEV and PD magnitude before and after XLPE cable samples were aged by impulses, different PD behavior was reported in literature [3], [9] and [10]. In [11] Densley et al. studied the features of PD that initiated under impulse. However, these results are based on polymeric material samples instead of cable samples. The PD initiation was investigated under AC with superimposed impulse voltage in [12], but similarly, the results are based on material samples. Consequently, PD initiation in a XLPE cable system under impulse and superimposed voltages still lacks insight. To address this our experiments are targeted to resolve the PD phenomena at the level of a laboratory cable model with an accessory defect, which becomes PD active under transient conditions.

A study of PD initiation under superimposed voltages in a MV XLPE

* Corresponding author.
E-mail address: j.wu-3@tudelft.nl (J. Wu).

https://doi.org/10.1016/j.ijepes.2020.106027
Received 12 February 2020; Accepted 15 March 2020
Available online 03 April 2020

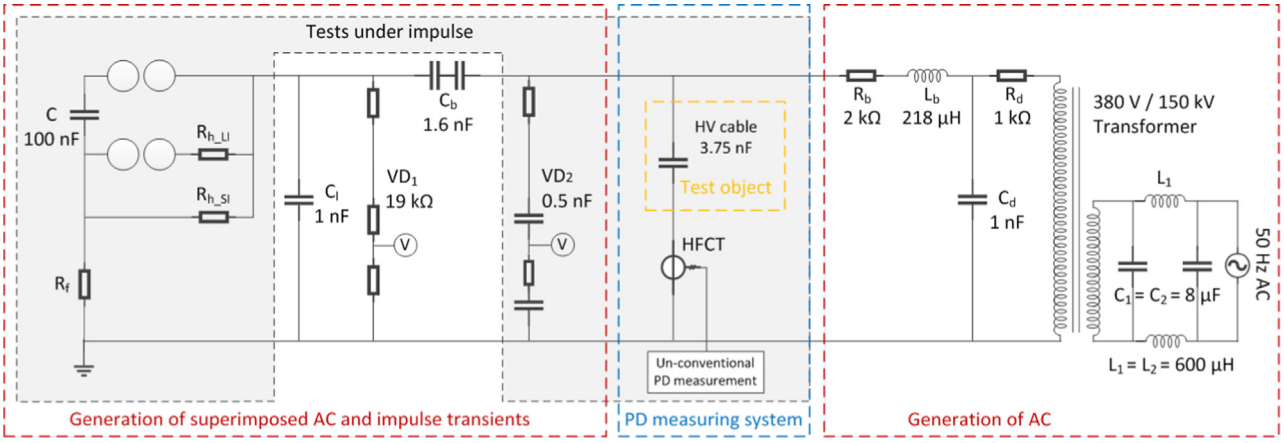

Fig. 1. Experimental setup for testing the HV cable system under superimposed transients.

cable model under lab conditions has been reported previously [13]. The results show that, superimposed voltage could initiate PD in the MV cable joint if an originally non-discharging insulation defect exists. In the current work, the PD initiation and development are investigated in a HV cable system under impulse and superimposed voltages. A 150 kV XLPE cable system with an artificial defect in the cable joint was tested under lab conditions. An adapted PD measuring system consisting of two HFCTs, band-pass filters, transient voltage suppressors and a digital oscilloscope was used (Section 2). The HV cable model was subjected to impulse voltage (Section 3) and superimposed (Section 4) voltages with different shapes. The measured PD signals were presented in phase-resolved PD patterns (PRPD), time-resolved pulse waveforms (TRPD), and usual PD parameters. By interpreting the PD behaviour, the effects of impulse and superimposed voltages on PD are derived and summarized in Section 5.

2. Experimental Set-Up

The circuit for investigating the effect of transients on the HV cable model consists of the HV cable system under test, the testing voltage supplies and the PD measuring system. Fig. 1 shows the schematic diagram of the experimental circuit. Values of all the elements are given except for the resistors in the impulse generator, which are adjusted according to the required waveforms of impulse voltages. A 150 kV XLPE insulated cable section with accessories was used as the test object for investigating the effects of transients. An unconventional PD measuring method was applied onto the cable joint to measure PD in the HV cable system. In the investigation, the HV cable system was tested under 50 Hz AC voltage, impulse voltage and superimposed voltage. For testing under 50 Hz AC voltage, the HV cable system was connected to a 380 V/150 kV AC transformer. For testing under impulse voltages, part of the circuit denoted by the grey area in Fig. 1 was connected. For testing under superimposed voltages, the entire circuit - including the AC transformer and the impulse generator - was connected. The blocking capacitor C_b enables the superposition of impulses on top of the AC voltage and reduces the stresses of the AC voltage on the capacitors of the impulse generator. In [14] the experimental setup and PD measuring system has been explained more in detail.

2.1. HV cable model

The 150 kV XLPE extruded power cable section is 16 m long in total. The total capacitance of the cable section is 3.75 nF. The HV cable is terminated with two outdoor-type terminations, named termination 1 and 2, and a pre-moulded joint which is located ten meters away from the termination 1. The cable is grounded at both cable terminations. Fig. 2 illustrates the structure of the cable joint.

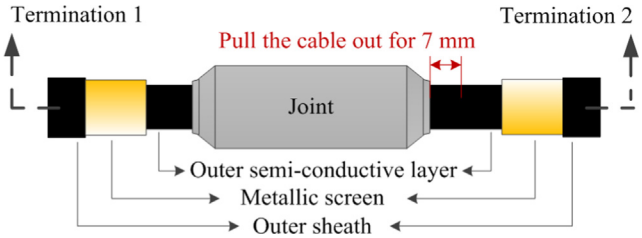

Fig. 2. HV cable joint and the artificial defect.

In order to produce partial discharges with AC PDIV above the operating voltage of the HV cable system, an artificial defect was created by manipulating the joint. The connector in the joint was prepared in such a way that the cable can be pulled out 7 mm of the joint at the side near to termination 2 (Fig. 2). In practice, this outbound cable displacement will not happen in a properly mounted cable joint. Whereas for laboratory testing, this defect can generate under AC voltage detectable partial discharges. With the defect dimension of outbound displacement of 7 mm, the PD inception voltages (PDIV) and extinction voltage (PDEV) were measured as 104 kV_{rms} and 90 kV_{rms} respectively.

2.2. Testing voltages

The HV cable model was tested under AC voltage, impulse voltage and superimposed transient voltage. In the impulse tests, impulse voltage waveforms with different peak values V_{peak}, front times T_f and times to half value T_h, as shown in Fig. 3a, were applied on the HV cable system. Fig. 3b gives an example of superimposed voltage waveforms. An impulse voltage with front time T_f and time to half value T_h rides on the AC wave crest with an AC peak of V_{ACpeak}, resulting in a total peak value V_{peak} of the test voltage. During the tests, the parameters T_f, T_h, V_{ACpeak}, V_{peak}, as well as the phase angle at which the impulse was superimposed on the AC voltage, were varied in order to study their effects on the PD behaviour of the HV cable system.

2.3. PD measuring system

Two identical high frequency current transformers (HFCT) were used as PD sensors to detect PD from the cable joint, with a gain of 3 mV/mA and a bandwidth of 100 kHz – 40 MHz [15]. These HFCTs were mounted at both ends of the joint with the same polarity, as shown in Fig. 4 to discern internal from external PD sources. In order to protect the oscilloscope against huge disturbances during the impulse application, a filter/suppressor protection unit, named 'Filter', was applied before the oscilloscope. The Filter consists of a band-pass filter with a

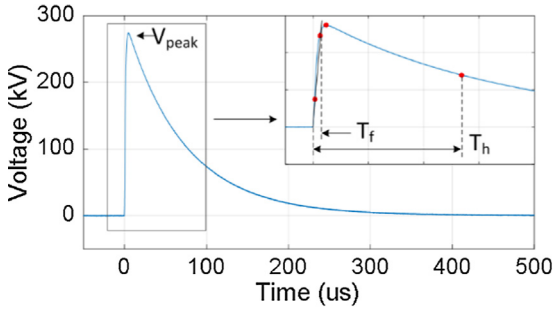

(a). Test voltage waveform of impulse voltage.

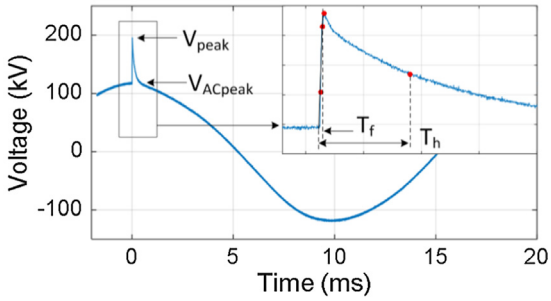

(b). Test voltage waveform of superimposed voltage.

Fig. 3. Test voltage waveforms.

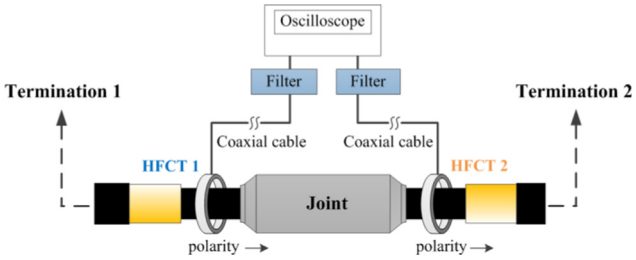

Fig. 4. Two HFCTs installed at two ends of cable joint.

bandwidth of 114 kHz – 48 MHz which attenuates the large disturbances of the impulse, and a transient voltage suppressor (TVS) together with a spark gap (SG) clipping the voltage off at 12 V. Such protection unit can attenuate but not eliminate the disturbance completely. In order to detect PDs during the impulse period, especially during the impulse front time, an extra band-pass filter with bandwidth of 1.38–90.2 MHz was added, which helped to further suppress the disturbances. However, the PD measuring system has an observation limitation: PD cannot be detected nor be separated from the disturbance signal during a certain period after applying the impulse, typically around 100–150 μs. This period is called the detection dead zone. The PD measuring system, in particular the 'Filter' unit and the detection dead zone, have been specifically explained in [14].

The PD signals captured by the two HFCTs were transmitted through two 20-meter identical coaxial cables and then acquired by a digital oscilloscope Tektronix MSO58. The sampling frequency was set to 1.25 GS/s. The PD acquisition channels were set with a bandwidth of 250 MHz and 1 MΩ internal impedance, but 50 Ω externally terminated for proper transmission line matching. A trigger level of 2.4 mV was selected. The acquired PD data were analyzed by PDflex [16]. The results were presented in phase-resolved PD patterns (PRPD), time-resolved PD pulses (TRPD) and typical PD parameters [17–19]. Clustering techniques were applied to separate PD from noise [20].

2.4. PD IN cable joint under AC voltage

Partial discharges, which are associated with the artificial defect in the cable joint, were firstly measured under AC voltage using the PD measuring system. The testing AC voltage was set at 108 kV_{rms} which is above the PDIV. Fig. 5 shows the measurement results in the form of PRPD patterns and TRPD pulse shapes. In Fig. 5c, for the PD pulse measured by HFCT 1, the peak amplitude of the first pulse of 11.2 mV is the PD magnitude of this PD event.

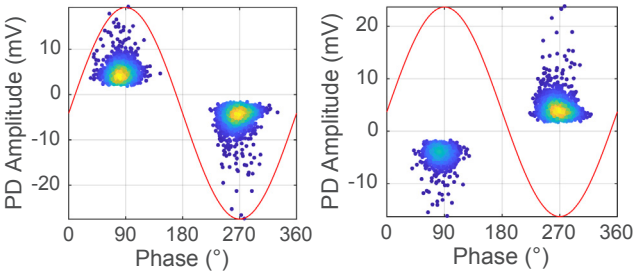

(a). measured by HFCT 1. (b). measured by HFCT 2.

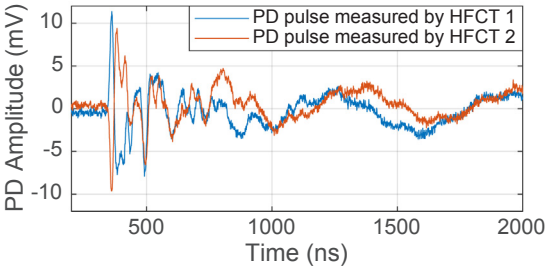

(c). TRPD pulse shapes of one PD event.

Fig. 5. PD measured at 108 kV_{rms} at the defect.

3. Defect PD activation by impulse voltages

HV impulse waves of relatively long and short impulse time as shown in Fig. 3a were applied on the HV cable model to simulate the effects of transients. For long impulse waves, the relatively long front time and tail time were chosen so that, on the one hand the impulses approach the standard switching impulse, and on the other hand the test circuit is able to withstand the impulses. The same applied to the short impulse waves, which were chosen so that the relatively short front and tail times approach the settings for the standard lightning impulse, while any circuit failure was avoided.

The impulse application generated a lot of disturbance which was also captured by the HFCTs. The TRPD pulse and polarity help to distinguish the PD signals from the disturbance signals. Fig. 6 shows the time-resolved pulse shapes of PD signal and disturbance signal measured by the HFCTs under impulses. The signals measured by the two HFCTs are always opposite in case of PD while these are in phase in case of disturbance.

3.1. Long impulse waves

The long Impulse waves applied on the HV cable system are given in Table 1. In test L1-L4, the applied impulses at four different peak amplitudes had the same time setting for the front time T_f of 410 μs and the tail time T_h of 2535 μs and. The peak value of the impulses V_{pk} increased with a step of 20% from L1 to L4. Partial discharges were measured during the impulse applications in test L1-L4, and the results are given in Fig. 7. In test L4-L6, the peak values of the applied impulses V_{pk} were kept the same at 274 kV, while the front times and the tail times were set shorter. Partial discharges measured in test L4-L6 are given in Fig. 8.

The PD occurrences during the entire impulses having the same time setting (T_f/T_h) for different peak values in tests L1 to L4 are illustrated in Fig. 7a. Consider the first PD initiated during the tail time of V_{L4}, shown as the red dot RD1 (RD stands for Reverse Discharge, Section

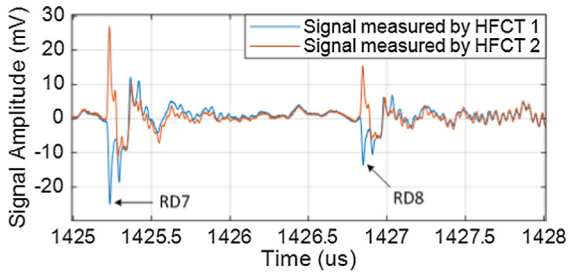

(a). Time-resolved pulse shape of PD signals.

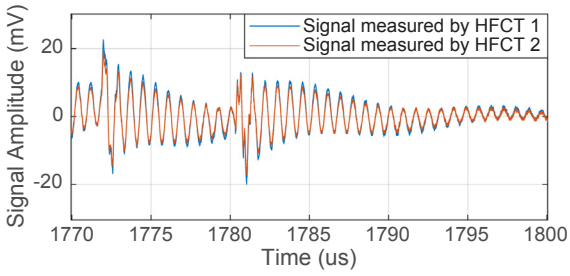

(b). Time-resolved pulse shape of disturbance signals.

Fig. 6. Time-resolved pulse shapes of PD and disturbance signals.

Table 1
Long Impulse Waves with their characteristics.

Tests	T_f/T_h [μs]	Peak value V_{pk} [kV]	Repeated test number
L1	410/2535	147	1
L2		176	1
L3		220	1
L4		274	6
L5	374/1612	274	6
L6	232/690	274	6

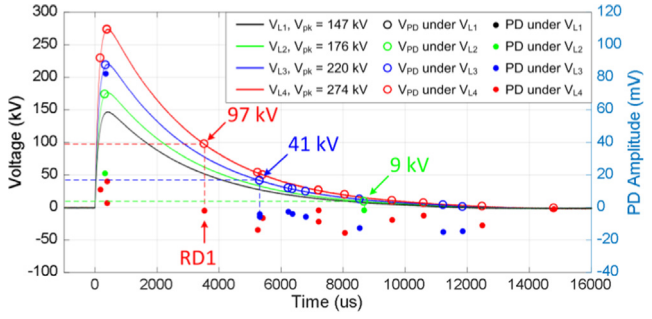

(a). PD occurrences during the entire impulses.

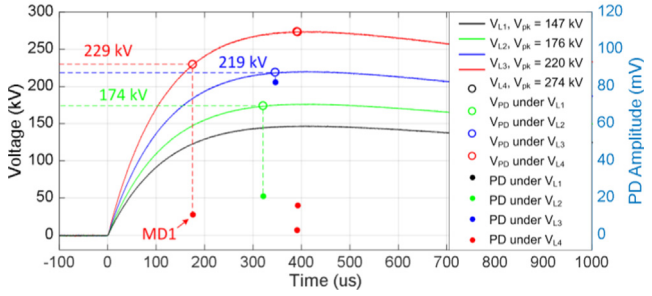

(b). PD occurrences during the front time.

Fig. 7. PD occurrence under long impulse waves with the time setting of T_f = 410 μs and T_h = 2535 μs for different peak values in test L1-L4.

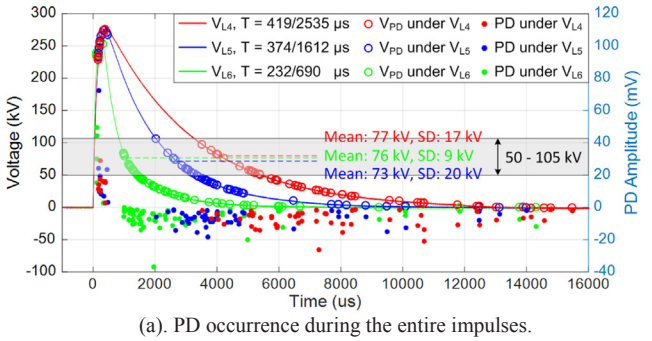

(a). PD occurrence during the entire impulses.

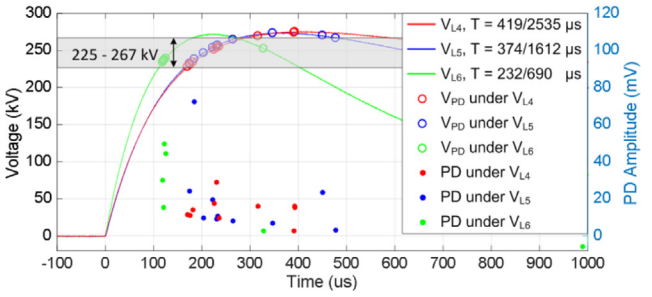

(b). PD occurrence during the front time.

Fig. 8. PD occurrence under long impulse waves with the same peak value of 274 kV and different time settings in test L4-L6.

3.2). It has a negative polarity with an amplitude of −7.1 mV. RD1 occurred at V_{L4} = 97 kV, indicated as the red circle on the wave tail. Similarly, the first PD initiated during the tail time of V_{L3} occurred at V_{L3} = 41 kV, and the first PD initiated during the tail time of V_{L2} occurred at V_{L2} = 9 kV. No PD has been observed under V_{L1}. For the same impulse front and half times, the higher the peak value of the impulse, the higher the voltage at which PD initiates during the impulse tail. From another perspective, the higher the peak value of the impulse, the earlier PD initiates. This can be seen from Fig. 7a as the PDs under V_{L4} (red dot) appear first, then the PDs under V_{L3} (blue[1] dot) ignite and at last the PDs under V_{L2} (green dot) occur.

The PD occurrence during the front time of the impulse is zoomed in and shown in Fig. 7b. The first PD detected during the front time of V_{L4} (red) is indicated as MD1 (MD stands for Main Discharge, Section 3.2), which has a positive polarity. Similarly, positive PDs initiate at voltages V_{L2} (green) and V_{L3} (blue) near to the impulse peaks. However, the initiation moments seem to be random.

In test L4-L6, PDs were measured during the entire impulses having the same peak value but three different time settings. Each test was repeated six times for each impulse front/half time setting, and the results of 18 tests are shown collectively in Fig. 8a. During the tail time of the impulse V_{L6} (green), the voltage level at which (negative) PD initiated for the six tests varies from 64 kV to 84 kV, which has an average is 76 kV (indicated as the dashed green line) with a standard deviation SD of 9 kV. The average PD initiation voltage under V_{L4} and V_{L5} is 77 kV (SD = 17 kV) and 73 kV (SD = 20 kV) respectively. The minimum and maximum PD initiation voltages among all the 18 tests are given as a range of 50–105 kV, indicated as the grey band in Fig. 8a. It shows that, the PD initiation voltage during the tail time of different impulse front/half time settings is comparable. In other words, during the tail of the impulse we observe for the three front/half times that negative PDs initiate when the impulse voltage decreases into the grey band. Accordingly, the PDs under V_{L6} (green) initiate at the earliest, and the PDs under V_{L4} (red) occur the latest in time. This can be seen from Fig. 8a as the group of green dots is leading in time compared to

[1] For interpretation of color in Figs. 7–9 and 11, the reader is referred to the web version of this article.

Table 2
Short Impulse Waves with their characteristics.

Tests	T_f/T_h [μs]	Peak value V_{pk} [kV]	Repeated test number
S1	3/56	150	1
S2		176	1
S3		226	1
S4		274	6
S5	3/26	274	6
S6	3/84	274	6
S7	3/174	274	6
S8	3/409	274	6
S9	3/782	274	6
S10	3/1630	274	6
S11	3/2006	274	6

the blue dots and red dots.

Similar sequence is observed for the PD occurrence during the front time, as shown in Fig. 8b. PDs initiate when the impulse voltage reaches a certain level near to the wave crest in the range of 225–267 kV under V_{L4}, V_{L5} and V_{L6}.

3.2. Short impulse waves

Same kind of tests were performed under short impulse waves. Table 2 gives the short impulse waves with their characteristics. Impulses with the same front/half time setting of T_f/T_h = 3/56 μs and different peak values were applied in test S1-S4. The peak values of the impulses increased with a step of 20% from S1 to S4. Impulses with the same peak value of 274 kV and different front/half time settings were applied in test S4-S11. Partial discharges measured in test S1-S4 and S4-S11 are shown in Fig. 9a and b respectively.

According to Densley [11], both Main Discharges (MD) during the front time and Reverse Discharges (RD) during the tail time of the impulse are supposed to be observed. However, due to the limitation of the PD measuring system [14], main discharges during the front time were not detectable as the front time is too short. Therefore, in the case of short impulse wave application, since the detection of main discharges is not possible, the analysis is restricted to the reverse discharges during the tail time.

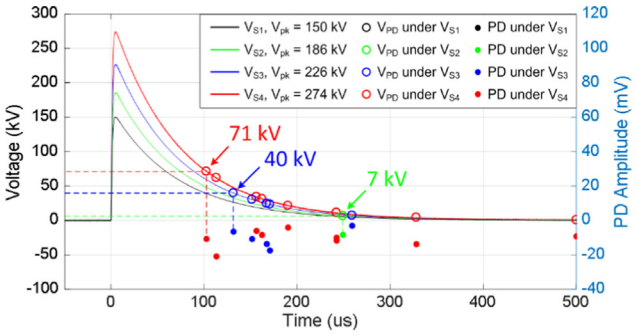

(a). PD occurrence under short impulse waves with the same time setting of T_f/T_h = 3/56 μs and different peak values in test S1-S4.

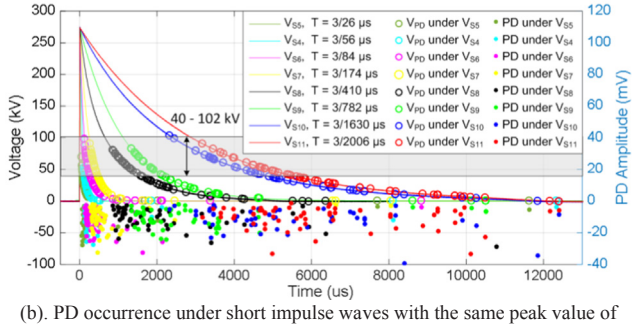

(b). PD occurrence under short impulse waves with the same peak value of 274 kV and different time settings in test S4-S11.

Fig. 9. PD occurrence under short impulses.

For the PD occurrence under short impulse waves with the same front/half time setting of T_f/T_h = 3/56 μs and different peak values in test S1-S4, similar sequences for PD initiation were observed as for long impulse waves as shown in Fig. 9a. Consecutively PDs under V_{S4} (red) initiated at V_{S4} = 71 kV, PDs under V_{S3} (blue) ignited at V_{S3} = 40 kV, and PDs under V_{S4} (green) occurred at V_{S4} = 7 kV. With the same impulse front/half time setting, the higher the peak value of the impulse, at higher voltage PDs initiate during the impulse tail.

The PD occurrence under short impulse waves with the same peak value and different front/half time settings is given in Fig. 9b. Each test was repeated for six times under each impulse waveform. During the tail time, the PD initiation voltages of all the 48 tests under V_{S4} to V_{S11} are in the range of 40–102 kV. When the impulse voltage decreases and falls into this range, PDs initiate. Therefore, the shorter the impulse front/half time setting, the earlier PDs initiate.

3.3. Discussion PD activation by impulses

The observation of different PD occurrence patterns under impulses at different front/half time settings and peak values can be explained by the internal electric field condition within the defect.

Fig. 10 shows schematic internal electric field conditions within the defect under V_{L1} to V_{L4} corresponding to test L1-L4. E_c is the enhancement of E_0, where E_0 is generated by the applied testing voltage, e.g. V_{L1} across the insulation thickness. Thus, E_c follows the wave shape of V_{L1}. E_q is created by the surface charges. The residual local field E_i is the sum of E_c and E_q, which drives the PD occurrence. The concept of E_i, E_c and E_0 have been detailed in [13]. During the front time of every impulse, as shown in Fig. 10a, PD initiates as soon as the local electric field E_i (dashed lines) reaches the PD inception field. After the first PD,

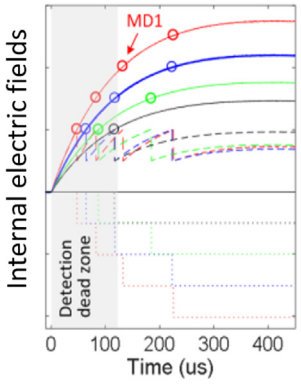

(a). during front time.

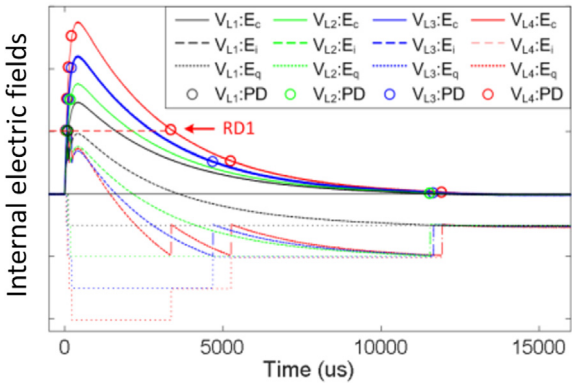

(b). during tail time.

Fig. 10. Schematic electric field conditions under long impulse waves in test L1-L4.

the local electric field E_i deviates from the background field E_c due to the discharge process and the arisen E_q, which has an opposite direction. Assume there is no charge decay, than E_q keeps constant between discharges. E_i increases with E_c again and when E_i reaches the PD inception field, PD reoccurs. However, such process doesn't match the PD measured in Fig. 7. This is due to the detection dead zone mentioned in Section 2.3. When applying long impulse waves, the detection dead zone is around 130 μs, which means that any PD occurring within 130 μs after the impulse may not be observed. Therefore, the first main discharge being observed is MD1. This can explain the random PD initiation in Fig. 7b, which actually occurred beyond the detection dead zone as shown in Fig. 10a. The development of the local electric field E_i further influences the PD initiation during the tail time. As shown in Fig. 10b, E_i of V_{L4} reaches the negative PD inception field firstly, which causes the first reverse discharge RD1. The first reverse discharge under V_{L3} appears later and under V_{L2} in the latest.

Fig. 10 gives a qualitative analysis of the electric field conditions with the assumption that there is no charge decay. In real defects, the charges deposited on the insulator surface from previous PD processes may decay by ion drift, diffusion through the gas and conduction along the insulator surface [21]. This will influence the E_q created by the charges and hereby the E_i. As a result, the PD occurrence will be slightly different and random, but still follow physics as explained above.

For impulses V_{L4} to V_{L6} corresponding to test L4-L6, due to the detection dead zone it is only possible to observe the PDs occurred after the dead zone, as shown in Fig. 11a. According to the schematic electric field conditions, E_i of V_{L6} starts to decrease firstly. Due to the biggest slope of V_{L6}'s tail wave, E_i of V_{L6} - shown as the green dashed line - reaches the negative PD inception filed earliest, which leads to the earliest PD occurrence under V_{L6}. E_i of V_{L4} and V_{L5} start to decrease almost at the same time. But V_{L4} has the smallest slope. Therefore, PDs under V_{L4} (red) occur at the latest. The voltages, at which PDs initiate

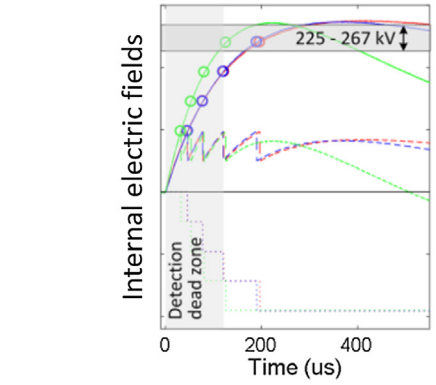

(a). during front time.

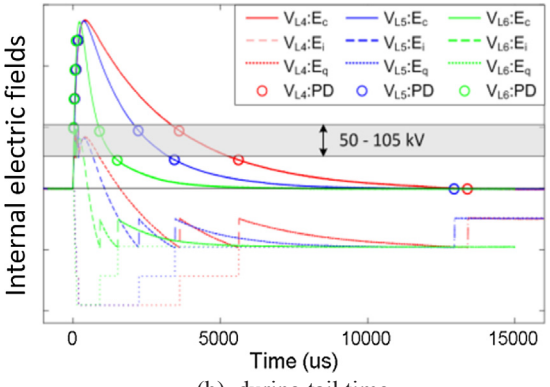

(b). during tail time.

Fig. 11. Schematic electric field conditions under long impulse waves in test L4-L6.

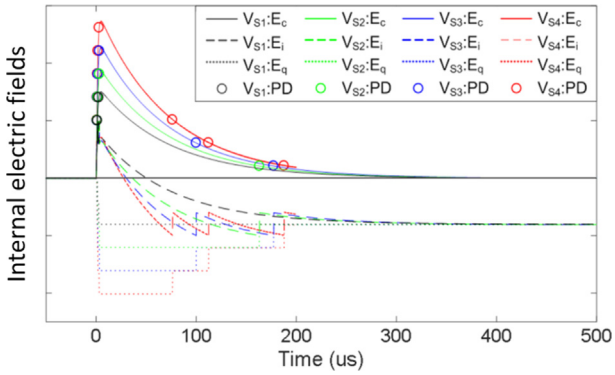

Fig. 12. Schematic electric field conditions under short impulse waves in test S1-S4.

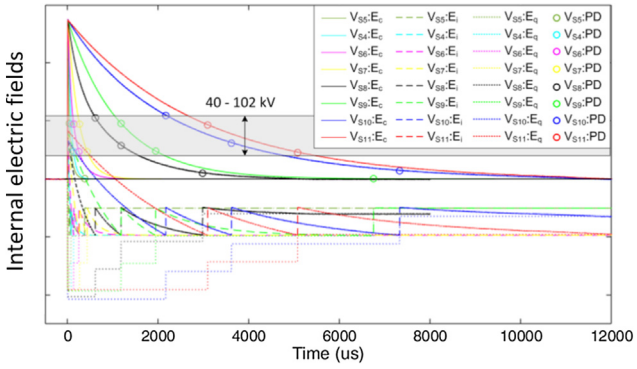

Fig. 13. Schematic electric field conditions under short impulse waves in test S4-S11.

under all the three front/half times based on the schematic local field conditions, fall into the range of 50–105 kV observed from experiments, as shown in Fig. 11b.

The electric field conditions of the defect under short impulse waves in test S1-S11 are shown in Figs. 12 and 13. For impulses V_{S1} to V_{S4} with the same front/half time setting and different peak values (Fig. 12), main discharges are supposed to occur during the front time as soon as the local electric field E_i reaches the PD inception field. During the tail time, due to the largest arisen E_q, the resulting E_i of V_{S4} reaches the negative PD inception field firstly, which causes the first reverse discharge. The first reverse discharge under V_{S3} occurs then and the one under V_{S2} initiates the latest. Moreover, with PD being initiated earliest, more PDs could occur under V_{S4} within the same impulse duration. The analysis is in accordance to the observation in Fig. 9a. However, in practice, since the front time is shorter than the dead zone, no main discharges during front time but only reverse discharges during the tail time were observed.

For impulses V_{S4} to V_{S11} with the same peak values and different front/half time settings (Fig. 13), the shorter the tail wave, the bigger the wave slope, the earlier E_i starts to decrease and reaches the negative PD inception field, the earlier PD initiates. The voltages, at which the first reverse discharges initiate under all the eight front/half times based on the schematic local field conditions, fall into the range of 40–102 kV observed from experiments, as shown Fig. 13.

4. Defect PD activation by superimposed voltages

The effect of transients on partial discharge initiation in the HV cable model was investigated for superimposed impulse voltage waveforms as shown in Fig. 3b. To observe the influence of different waveforms the AC and impulse voltage combinations listed in Table 3 were applied to the cable system. The parameter *Ratio* is the ratio of the

Table 3
Tests on HV Cable under Superimposed Voltages.

Impulse T_f/T_h [μs]	AC [kV_{rms}]	Ratio	φ [°]	PDIV [kV_{rms}]	Test	Max PD magnitude [mV]	Total PD number	Duration [s]	PD probability
3/91	88	1.8	0	97	1	43.2	180	2.92	6/6
		1.7	0		2	27.0	110	1.87	6/6
		1.7	0	104	3	64.0	95	1.20	6/6
		1.6	30		4	106.6	61	1.13	6/6
		1.2	60		5	56.9	64	0.71	1/6
		1.0	90		6	–	–	–	0/6
		1.7	180		7	51.8	124	1.29	6/6
		1.4	60		8	48.7	47	0.69	6/6
	94	1.8	0	97	9	73.9	1480	14	2/2
		1.7	0		10	67.4	933	7.76	6/6
		1.7	0	104	11	72.5	443	3.17	6/6
		1.7	180		12	73.8	301	2.87	6/6
93/845	88	1.6	0	97	13	132.8	165	1.9	6/6
		1.5	30		14	45.2	23	0.86	6/6
		1.1	60		15	–	–	–	0/6
		0.7	90		16	–	–	–	0/6
		1.4	0		17	37.9	11	0.06/1.12	6/6

total peak voltage V_{peak} to the AC voltage peak value V_{ACpeak}. φ is the phase angle at which the impulse is superimposed on AC. The PDIVs were always measured just before the tests, which confirmed that the cable model was PD free at operating voltage before the test. Each test consisted of six same measurements, in which the same specific waveforms were applied on the HV cable model and partial discharges were measured. For each test, the most representative result of the six measurements is summarized in Table 3. The Max PD magnitude in Table 3 is the maximum PD magnitude among the measured PD events in each test. The total PD number is the total number of PDs measured after applying the superimposed transients. Duration is the time duration of PD occurrence counted from the moment of impulse application to the moment the last PD observed. PD probability states the number of tests in which PDs initiated by the superimposed transients out of six tests. The measurement results given in Table 3 are shown in Fig. 14.

4.1. Partial discharge initiation under superimposed transient

In most of the tests, partial discharges were initiated by the superimposed transients and persisted under AC voltage for a certain period of time. Although the PD behavior is different under different transient waveforms, the principle of the PD initiation is related to the electric field conditions within the defect. Test 13 with long impulse wave and test 2 with short impulse wave superimposed on the AC wave are described in detail in the following.

Fig. 14l depicts the measurement result of test 13. Since the applied impulse has a long front time, it was possible to observe the main discharge, which initiated as soon as the impulse was applied (Fig. 14l). When the voltage turned to the negative cycle, several negative discharges occurred. Fig. 15 shows the observed main discharge and the first negative discharge by their TRPD pulse shapes.

The physical process of PD initiation determined by the electric field condition within the defect is described in Fig. 16. Without considering the charge decay and the trapped charges (Fig. 16a), the first main discharge initiates as soon as the local field E_i reaches the inception field E_{inc} at the impulse rising phase. After the discharge process, the charges deposited on the defect surface creates an opposite E_q, which deviates E_i from the background field E_c. When the voltage turned to the negative cycle, very soon E_i reaches the negative inception field $-E_{inc}$ and the negative discharges occur. After the positive discharge occurred in the next positive cycle, E_i regresses to E_c and no more PD occurs.

In practice, the charges left on the defect surface decay with time before the next discharge event occurs. Thus, instead of being constant, the created E_q decreases. This will influence the resulting E_i and PD occurrence. As observed in Fig. 16b, following the negative discharges in the first negative cycle, two positive discharges occur in the positive cycle and a negative E_q is left. With the decreasing E_q, E_i could reach the $-E_{inc}$ again leading to another discharge. And then the discharges reoccur. This is in accordance with the observation in the test (Fig. 14l). Moreover, apart from the charges deposited on the defect surface, there are also charges that are trapped on the surface with a certain energy level. If they obtain enough energy, they could escape from the traps and become free charges, which are potential first electrons for partial discharges to occur. If they stay in traps on the surface, they may also create a tiny field E_q which keeps E_i deviating from E_c.

In test 13, the PD activity lasted for around two seconds. The PD extinction might be caused by the lack of the first free electron and insufficient local field. With more PDs occurring in the defect, the charges will increase the conductivity of the defect surface, which leads to a faster charge decay. With faster charge decay, the created E_q after a PD event will decrease faster so that no more free charges are available as the first free electron. Without the E_q created by the deposited charges, the tiny field created by the trapped charges is not enough to drive E_i reaching E_{inc}. As a consequence, the discharge cannot reoccur.

In test 2, the superimposed impulse has a short front time of 3 μs, which is within the dead zone of the PD measuring system. Therefore, it is not possible to detect main discharges during the impulse. As shown in (Fig. 14b), the first detected PD is in the negative cycle. The main discharge, which is supposed to occur, can be seen from the schematic electric field condition (Fig. 17). Without considering the charge decay (Fig. 17a), main discharges initiate when the impulse is applied. During the first negative cycle, discharges reoccur for several times. Since no charge decay is considered, the field E_q created by charges keeps constant between two PD pulses, and reaches or crosses zero after several PDs. With such low E_q, the local field E_i cannot reach the inception field E_{inc}. Thus, PD extinguishes. If considering the charge decay (Fig. 17b), the field E_q decreases between every two PD pulses. Due to the slow charge decay and the very short interval between two PDs, the change in E_q is not obvious in Fig. 17b. However, after several PDs, the accumulated charge decay processes result in a positive E_q, which makes the local field E_i reaches the inception field E_{inc}. Consequently, PD persist under AC voltage. Similar to the case in test 13, the PD activity was recorded for around two seconds.

Since the partial discharge process is a dynamic process, and the real field conditions in the defect are influenced by many other factors, such as the defect dimension and shape, the gap composition in the defect, the aging condition of the insulation surface etc., the schematic electric field conditions cannot completely reveal the real field conditions within the defect. However, they are very helpful for

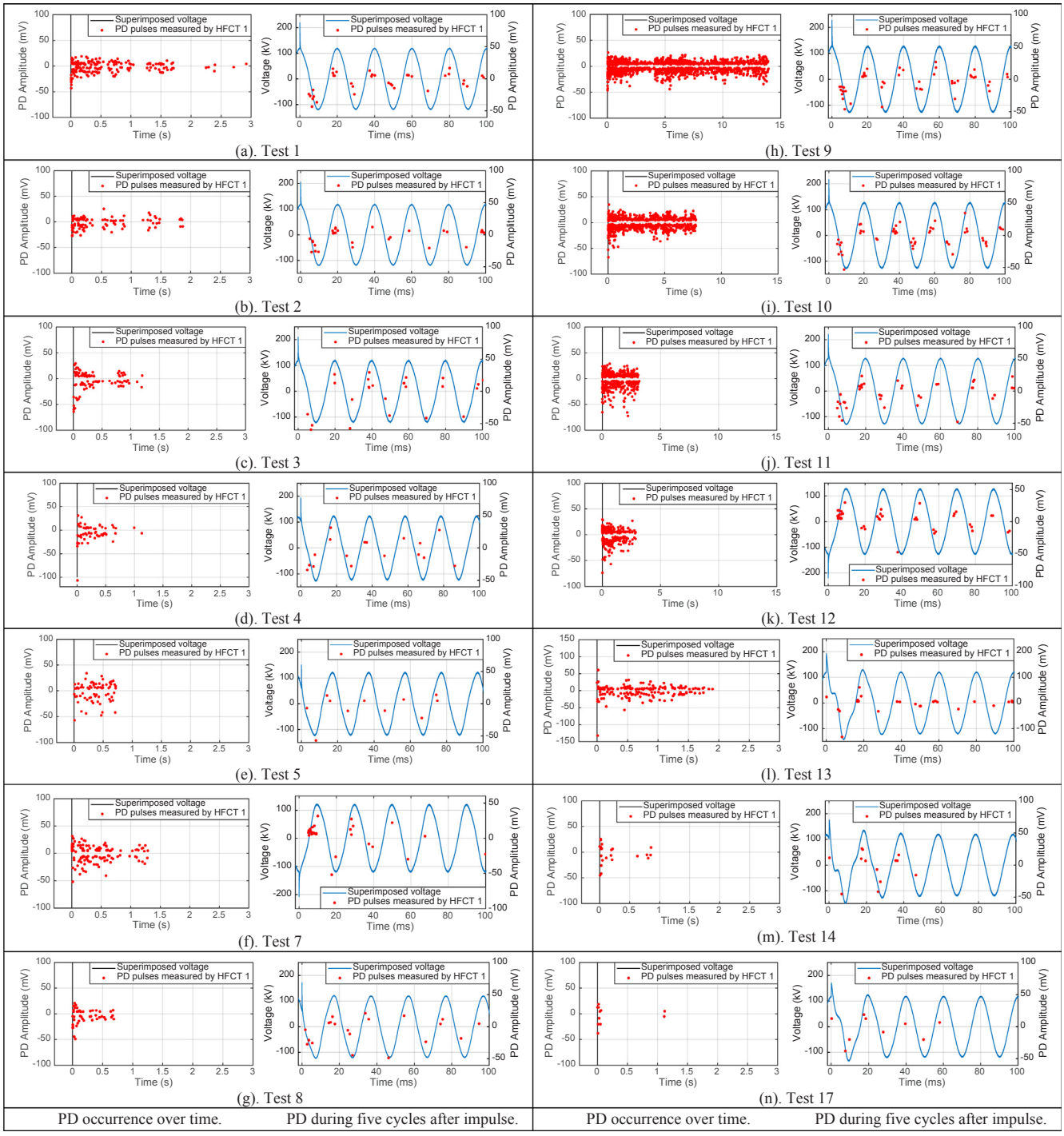

Fig. 14. PD occurrence due to impulses superimposed on AC voltages.

understanding the physical process of partial discharges under the transients.

The results presented in Table 3 and Fig. 14 show that, the superimposed transients could initiate partial discharges in the cable system. After the transient, the PD behavior is influenced by the ongoing AC voltage which determines the background field E_c, as well as the surface charges left by previous discharges process which determines the E_q. The influence of different waveforms on the PD behavior is to be discussed in the following section.

4.2. Influence of different ratios

In test 1 (Fig. 14a) and test 2 (Fig. 14b), the short impulses with T_f/T_h = 3/91 μs were superimposed on the same AC voltage of 88 kV_{rms} at 0° with different ratios of 1.8 and 1.7 respectively. The PDIV were measured before each test as 97 kV_{rms}. As discussed before, partial discharges were supposed to initiate during the impulse. However, due to the dead zone of the PD measuring system, only PDs beyond the dead zone are detectable. For this reason, only PDs from the first negative cycle after the impulses are observed. In both tests, the number and magnitude of PDs which occurred during the first cycle right after the impulses are relatively high. The maximum PD magnitudes as shown in

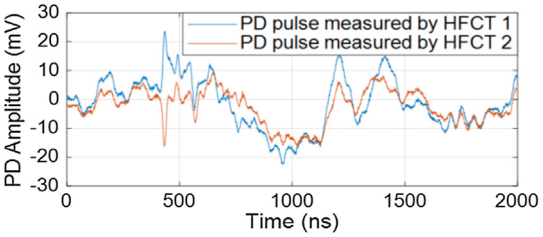

(a). the first main discharge.

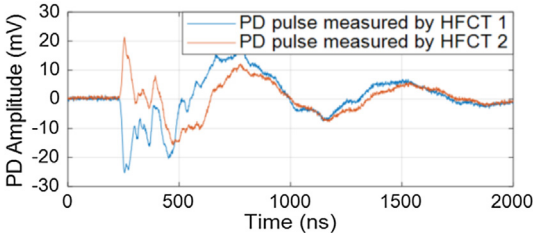

(b). the first negative discharge.

Fig. 15. TRPD pulse shapes of PDs measured in test 13.

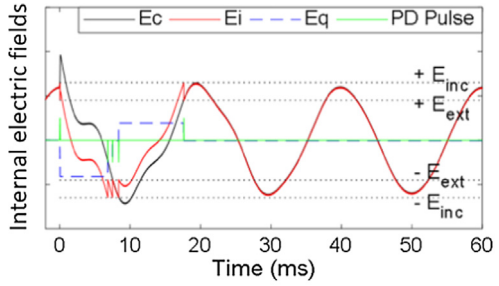

(a). without considering charge decay and the trapped charges.

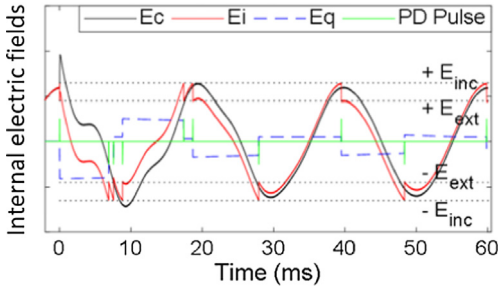

(b). considering charge decay and the trapped charges.

Fig. 16. Schematic electric field conditions in test 13.

Table 3 occurred in the first cycle in both tests. With time, it was observed that both the PD magnitude and the PD number per cycle, i.e. the PD repetition rate, decrease until PD extinguished. In both tests, the PD activities lasted for a few seconds. In test 1, with waveform ratio 1.8, the PD activity lasted longer (longer duration) and more PDs occurred (larger PD number) during this process than in test 2. Such difference in PD behavior is seen as a result of different field conditions caused by the different ratios. This is illustrated in Fig. 18. With higher ratio, a larger impulse is superimposed on AC voltage, which results in a longer period of time during which the applied voltage is higher than the PDIV. This gives more chances for more PDs to occur in a short time. In addition, those consecutively occurred PD events would generate more charges which will contribute to a larger E_q. This would further lead to a larger E_i and therefore to more PD events. Consequently, more charges are accumulated before decaying and recombination. Those charges enable PD activity to persist for a longer time under AC voltage. Therefore, the impulse determines the early initiated PDs, especially during the first

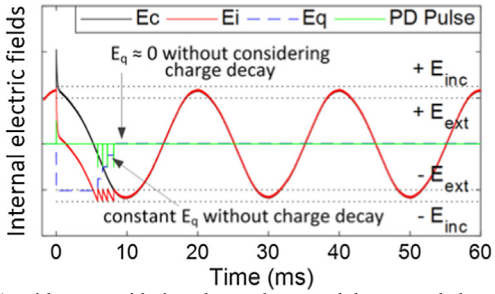

(a). without considering charge decay and the trapped charges.

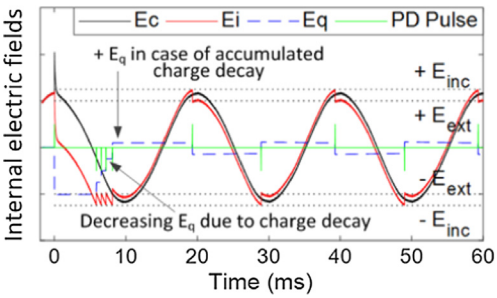

(b). considering charge decay and the trapped charges.

Fig. 17. Schematic electric field conditions in test 2.

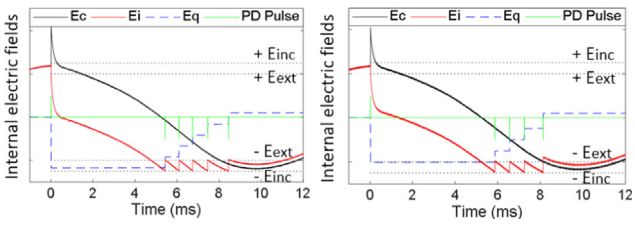

(a). test 1, ratio=1.8. (b). test 2, ratio=1.7.

Fig. 18. Schematic electric field conditions in test 1 and test 2 for different ratios.

cycle after the impulse. Those early initiated PDs further influence the PD behavior under AC voltage.

A similar effect of the ratio value on partial discharges is observed with higher AC voltage in test 9 vs. test 10, and with longer impulses in test 13 vs. test 17. In test 9 and test 10 (Fig. 14h and i), the short impulses were applied on an AC voltage of 94 kV_{rms} with ratio of 1.8 and 1.7 respectively. With ratio of 1.8, more PDs occurred, and the PD activity lasted longer. In test 13 and test 17 (Fig. 14l and Fig. 14n), longer impulses with T_f/T_h = 93/845 μs were applied on an AC level of 88 kV_{rms}. Main discharges are observed during the impulse. With a ratio of 1.4 in test 17, very few PDs occurred, resulting in a small PD number and shorter duration.

4.3. Influence of different phase angles

In test 3 to test 6, the same impulses were superimposed on the AC voltage at phase angles of 0°, 30°, 60° and 90° respectively. For the same impulse amplitude, this results in different ratios as shown in Table 3. When the impulse was applied at 0° in test 3 and at 30° in test 4, PD were always initiated by the impulse for all the repeated six tests (PD occurrence = 6/6). PD occurred in test 3 lasted slightly longer than that in test 4, and the PD density is also slightly higher than that in test 4 (Fig. 14c and d). However, when the impulse was applied at 60° in test 5, in only one out of six tests ((Fig. 14e) PDs occurred (PD occurrence = 1/6). And with 90° in test 6, no PD were initiated by the impulses among all the repeated tests (PD occurrence = 0/6).

Considering the schematic electric field conditions, although they

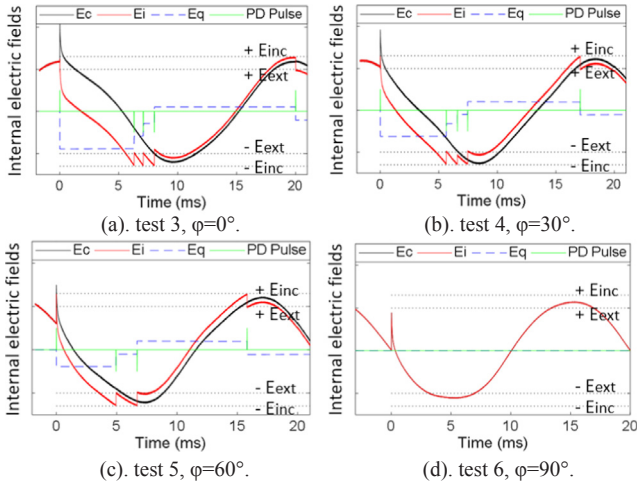

Fig. 19. Schematic electric field conditions in test 3 to test 6 with different phase angles.

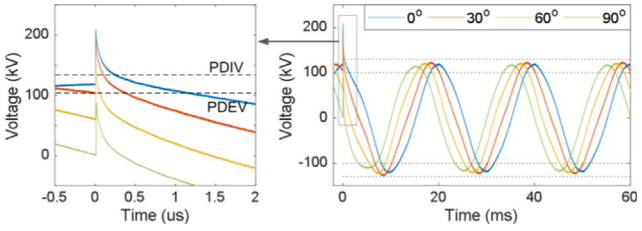

Fig. 20. Overvoltage vs. PDIV in test 3 to test 6.

are slightly different under waveforms with 0° (Fig. 19a) and 30° (Fig. 19b), they cause similar PD events during the first cycle after the impulses. With an angle of 60°, less PDs occurred (Fig. 19c). With an angle of 0°, no PD could occur (Fig. 19d).

In test 3 to test 6, both the phase angle and the ratio vary. Between these two parameters, we assume that the ratio, more precisely the overvoltage value, is dominantly affecting the PD occurrence. This is illustrated in (Fig. 20). For all the four tests, the PDIV was measured the same as 104 kV_{rms}. When the impulse was applied at a larger phase angle, a smaller peak value was obtained. Consequently, the period of time the voltage being higher than the PDIV is shorter, or the voltage even cannot reach the PDIV. In this case, PD will not, or only have small chance to occur. This has been observed in test 5 and test 6. It is worth noting that, with 60° the overvoltage also exceeds the PDIV for a very short time in Fig. 20, which is still supposed to initiate PDs. However, it is quite possible that the first free electron for PD initiation cannot be available during this short time. Then PD losses the chance to initiate. Thus, for only one out of six tests PDs occurred in test 5.

In order to further confirm the assumption that the overvoltage value is the dominant parameter of PD occurrence, in test 8 the impulse was applied at the same phase angle of 60° as in test 5, while the resulting ratio is 1.4, being higher than that of 1.2 in test 5. In this case, PD were observed in all of the six tests (PD occurrence = 6/6). One measurement is shown in Fig. 14g. Hereby we can conclude that, the dominant parameter which influences the PD occurrence is the ratio, or the total overvoltage value.

The same phenomenon was observed in test 13 to test 16 with longer impulses. PDs were always initiated (PD occurrence = 6/6) by the impulses when they were applied at 0° and 30°, while no PD was observed with phase angles of 60° and 90° (PD occurrence = 0/6). PD that occurred in test 13 lasted longer than those in test 14, and the PD density is also much higher than that in test 14 (Fig. 14l and m).

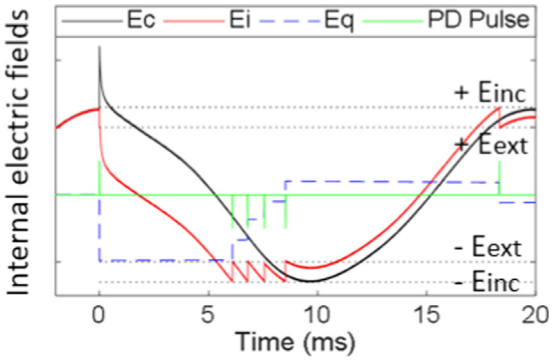

Fig. 21. Schematic electric field conditions in test 11 with AC of 94 kV_{rms}.

4.4. Influence of different PDIV values

The voltage waveforms applied in test 2 and test 3 were exactly the same, while the PDIV values measured before the tests were different. With lower PDIV at 97 kV_{rms} in test 2, it is easier for the voltage to reach the PDIV value. Therefore, more PDs were initiated in the first cycle but with lower amplitude (Fig. 14b). The schematic electric field condition is seen in Fig. 18b. However, the PD activity lasted longer in test 2. With higher PDIV value in test 3, less PDs with higher amplitude occurred, but the PD activity lasted shorter (Fig. 14c). The schematic electric field condition is seen in Fig. 19a.

Similar phenomenon is observed in test 10 (Fig. 14i) and test 11 (Fig. 14j), where the AC voltage for both tests were set as 94 kV_{rms}.

4.5. Influence of different AC levels

If the PDIV value is kept the same, with all the other parameters the same but higher AC voltage, it is also easier for the voltage to reach the PDIV value and then initiate more PDs. The effect of AC level can be seen in test 1 vs. test 9, test 2 vs. test 10, and test 3 vs. test 11. In each pair of tests, under the waveform with higher AC voltage level, more PDs with higher amplitude initiated in the first cycle, and the PD activities lasted for longer time. The schematic field conditions in test 3and test 11 are shown in Figs. 19a and 21.

4.6. Influence of different impulse polarities

In test 7, the same impulse as in test 3 was applied but with negative polarity and on the negative AC crest. Beside more PDs occurring in test 7, similar PD behaviour has been observed as in test 3. In test 11 and test 12 with higher AC voltage, the PD behaviour under positive impulse and negative impulse are similar as well. As a conclusion, the polarity of the impulse will not have an impact on the PD behaviour.

5. Conclusions

In this work, partial discharges were investigated in a 150 kV XLPE cable model under transient situations. An artificial defect was introduced in the cable joint in order to generate partial discharges. An unconventional PD measuring system was used to measure PDs during and after the impulse application. The HV cable system was subjected to pure impulse voltages and superimposed voltages separately.

The PD measurement results obtained from the pure impulse tests show that, the impulse voltage can initiate partial discharges with sufficient voltage level. Several main discharges initiated during the front time of the impulses. More reverse discharges occurred during the tail time of the impulses until the impulse finished. For the impulse voltages with the same front/half time setting (T_f/T_h), the higher the peak value, the earlier PD would initiate and the more PDs would occur during the entire impulse. While for the impulse voltages with the same

peak value and different front/half time settings, the shorter the impulse, the earlier PD would initiate. However, for the tested waveforms, the front/half time setting doesn't play a significant role in the number of occurring PDs. As a conclusion, the peak value of the impulse voltage has more significant effect on partial discharges than the impulse front/half time setting.

The PD measurement results obtained from the superimposed transients show that, partial discharges can be initiated by the superimposed transients under certain conditions. When the impulse was applied, main discharges with the same polarity as the impulse were firstly initiated during the front time of the applied impulse. After the impulse finished, the initiated PDs were sustained by the AC voltage. The parameters of the superimposed transients influence the PD behaviour: the higher the peak overvoltage value (in other words, the ratio), the higher number of PDs occurs, some of which PD would persist for a longer time under AC voltage. When the same impulse was superimposed on the AC voltage with a certain phase angle, the larger the phase angle (the farther the impulse is from the AC crest), the less probability and the less numbers of PDs would occur. With higher PDIV, less PDs with higher amplitude occurred. And higher AC voltage level may lead to more PDs with higher amplitude initiated in the first cycle and longer duration of PD activities. Lastly, the polarity of the impulse does not have an impact on the PD behaviour.

The influence of the superimposed transients on PD behaviour can be explained by the electric field conditions within the defect. Basically, the overvoltage of the impulse will initiate a group of PDs with higher number and magnitude during the first cycle, which leave many charges on the surface of the defect and cause a change in the electric field condition. The generated charges will increase the probability of PD occurrence by contributing to the local field and providing free electrons. This will further influence the PD activity persisting under AC voltage

Declaration of Competing Interest

The authors declare that they have no known competing financial interests or personal relationships that could have appeared to influence the work reported in this paper.

Acknowledgment

Authors would like to thank TenneT B.V. of the Netherlands for funding this project.

References

[1] CIGRÉ WG C4.502. Power system technical performance issues related to the application of Long HVAC cables. Technical Brochure 556, Paris, October 2013.
[2] CIGRÉ WG B1.30. Cable systems electrical characteristics. Technical Brochure 531, Paris, April 2013.
[3] CIGRÉ WG B1.10. Update of service experience of HV underground and submarine cable systems. Technical Brochure 379, Paris, April 2009.
[4] CIGRÉ WG B1.47. Implementation of long AC HV and EHV cable systems. Technical Brochure 680, Paris, March 2017.
[5] Maanen V, Gl D, Meijer S. Failures in underground power cables – return of experience. In: 9th International Conference on Insulated Power Cables, Jicable'15, Versailles 21–25 June 2015.
[6] Hoogendorp G. Steady State and transient behavior of underground cables in 380 kV transmission grids. Delft University of Technology; 2016.
[7] Densley J. Ageing mechanisms and diagnostics for power cables - an overview. IEEE Electr Insul Mag 2001;17(1):14–22.
[8] Hartlein R, et al. Applying Diagnostics to Enhance Cable System Reliability (Cable Diagnostic Focused Initiative, Phase II). 1255949; 2016.
[9] Cao L, Grzybowski S. Accelerated aging study on 15 kV XLPE and EPR cables insulation caused by switching impulses. IEEE Trans Dielectr Electr Insul 2015;22(5):2809–17.
[10] Xu L, et al. The degradation of 10kV XLPE cable accessories under switching impulses. 2018 12th international conference on the properties and applications of dielectric materials (ICPADM). 2018. p. 463–6.
[11] Densley RJ, Salvage B. Partial discharges in gaseous cavities in solid dielectrics under impulse voltage conditions. IEEE Trans Elect Insul 1971;EI-6(2):54–62. https://doi.org/10.1109/TEI.1971.299155.
[12] Densley RJ. Partial discharges in electrical insulation under combined alternating and impulse stresses. IEEE Trans Elect Insul 1970;EI-5(4):96–103. https://doi.org/10.1109/TEI.1970.299117.
[13] Wu J, Rodrigo Mor A, Smit JJ. The effects of superimposed impulse transients on partial discharge in XLPE cable joint. Int J Electr Power Energy Syst 2019;110:497–509.
[14] Wu J, Rodrigo Mor A, van Nes PVM, Smit JJ. Measuring method for partial discharges in a high voltage cable system subjected to impulse and superimposed voltage under laboratory conditions. Int J Electr Power Energy Syst 2020;115:105489.
[15] On-line Partial Discharge Products and Test Services | HVPD. [Online]. Available: https://www.hvpd.co.uk/. [Accessed: 08-Mar-2019].
[16] Partial discharges software - PDflex: PD parameters and clustering. PDFlex - Unconventional partial discharge analysis. [Online]. Available: http://pdflex.tudelft.nl/. [Accessed: 28-Aug-2018].
[17] Rodrigo Mor A, Heredia LCC, Munoz FA. Estimation of charge, energy and polarity of noisy partial discharge pulses. IEEE Trans Dielectr Electr Insul 2017;24(4):2511–21.
[18] Rodrigo Mor A, Morshuis PHF, Smit JJ. Comparison of charge estimation methods in partial discharge cable measurements. IEEE Trans Dielectr Electr Insul 2015;22(2):657–64.
[19] Rodrigo Mor A, Castro Heredia LC, Muñoz FA. New clustering techniques based on current peak value, charge and energy calculations for separation of partial discharge sources. IEEE Trans Dielectrics Electrical Insul 2017;24(1):340–8.
[20] Rodrigo Mor A, Muñoz FA, Wu J, Heredia LCC. Automatic partial discharge recognition using the cross wavelet transform in high voltage cable joint measuring systems using two opposite polarity sensors. Int J Electr Power Energy Syst 2020;117.
[21] Niemeyer L. A generalized approach to partial discharge modeling. IEEE Trans Dielectr Electr Insul 1995;2(4):510–28.

Jiayang Wu was born in Nanjing, China in 1988. She received the BSc degree in electrical engineering from the Southeast University, Nanjing, China, in 2010, and the MSc degree in electrical power engineering from the RWTH Aachen University of Technology, Aachen, Germany in 2013. She received her Ph.D degree in the Electrical Sustainable Energy Department at Delft University of Technology, Delft, The Netherlands in 2020 with her research focused on the effects of transients on the high voltage cable systems. She is currently a consultant in DNV GL, Arnhem, the Netherlands.

Armando Rodrigo Mor is an Industrial Engineer from Universitat Politècnica de València, in Valencia, Spain, with a Ph.D. degree from this university in electrical engineering. In Spain, he joined and later led the High Voltage Laboratory and the Plasma Arc Laboratory of the Instituto de Tecnología Eléctrica in Valencia, Spain. Since 2013 he is an Assistant Professor in the Electrical Sustainable Energy Department at Delft University of Technology, in Delft, Netherlands. His research interests include monitoring and diagnostic, sensors for high voltage applications, high voltage engineering, space charge measurements and HVDC.

Johan J. Smit is professor at the Delft University of Technology (The Netherlands) in High Voltage Technology and Management since 1996 and emeritus since 2015. After his graduation in experimental physics he received his PhD degree from Leiden University in 1979. After his research in cryogenic electromagnetism at the Kamerlingh Onnes Laboratory, he was employed as T&D research manager at KEMA's laboratories in Arnhem-NL for 20 years. Furthermore, he was director of education in electrical engineering, supervisory board member of the power transmission company of South Holland, and CEO of the asset management foundation Ksandr for 10 years. In 2003 he was general chairman of the International Symposium on HV Engineering in Delft. He is TC-honorary member of CIGRE and past chairman of CIGRE D1 on Materials & Emerging Technologies. Currently he is convener of the area Substation Management for CIGRE B3 and he holds the international chair of Technical Committee IEC112 on Electrical Insulation Systems.